ARL-TR-10139 ● JULY 2025

DEVCOM ARMY RESEARCH LABORATORY

High-Throughput Evaluation of Nanophase Separation Sintering for Alloy Design

by Philip E. Goins and Heather A. Murdoch

NOTICES

Disclaimers

The findings in this report are not to be construed as an official Department of the Army position unless so designated by other authorized documents.

Citation of manufacturer's or trade names does not constitute an official endorsement or approval of the use thereof.

Destroy this report when it is no longer needed. Do not return it to the originator.

ARL-TR-10139 ● JULY 2025

High-Throughput Evaluation of Nanophase Separation Sintering for Alloy Design

Philip E. Goins and Heather A. Murdoch
DEVCOM Army Research Laboratory

REPORT DOCUMENTATION PAGE

1. REPORT DATE	2. REPORT TYPE	3. DATES COVERED	
		START DATE	END DATE
July 2025	Technical Report	10-1-2022	3-1-2025

4. TITLE AND SUBTITLE
High-Throughput Evaluation of Nanophase Separation Sintering for Alloy Design

5a. CONTRACT NUMBER	5b. GRANT NUMBER	5c. PROGRAM ELEMENT NUMBER
5d. PROJECT NUMBER	**5e. TASK NUMBER**	**5f. WORK UNIT NUMBER**

6. AUTHOR(S)
Philip E. Goins and Heather A. Murdoch

7. PERFORMING ORGANIZATION NAME(S) AND ADDRESS(ES)
DEVCOM Army Research Laboratory
ATTN: FCDD-RLA-MF
Aberdeen Proving Ground, MD 21005

8. PERFORMING ORGANIZATION REPORT NUMBER
ARL-TR-10139

9. SPONSORING/MONITORING AGENCY NAME(S) AND ADDRESS(ES)	10. SPONSOR/MONITOR'S ACRONYM(S)	11. SPONSOR/MONITOR'S REPORT NUMBER(S)

12. DISTRIBUTION/AVAILABILITY STATEMENT
DISTRIBUTION STATEMENT A. Approved for public release: distribution unlimited.

13. SUPPLEMENTARY NOTES

14. ABSTRACT
Many promising materials from a theoretical performance perspective are designed without a pathway for scalable production in mind, which leaves any actual gains unrealizable. To avoid this pitfall, cost-saving and force-multiplying tools to identify scalable materials before extensive and expensive laboratory testing can and should be developed. In this work, we have developed a tool to rapidly screen alloys as candidates for a recently developed nanophase sintering approach, which enables pressure-free, near-net-shape full consolidation of materials that would normally require much higher, often prohibitive, processing temperatures, while preserving desirous microstructure and properties. This tool, built using Python and the Thermo-Calc Software Development Kit, can be used to rapidly down-select and optimize alloy compositions that are amenable to this state-of-the-art approach; thus, significantly reducing the risk of poor processing in select alloy systems using thermodynamic and kinetic considerations. This package is designed to be easily integrated into any alloy design program that seeks to down-select or optimize alloy composition for a given application.

15. SUBJECT TERMS
Sciences of Extreme Materials, sintering, solid-state processing, computational materials science, integrated computational materials engineering, alloy design, optimization

16. SECURITY CLASSIFICATION OF:			17. LIMITATION OF ABSTRACT	18. NUMBER OF PAGES
a. REPORT	b. ABSTRACT	C. THIS PAGE		
UNCLASSIFIED	UNCLASSIFIED	UNCLASSIFIED	UU	26

19a. NAME OF RESPONSIBLE PERSON	19b. PHONE NUMBER *(Include area code)*
Philip E. Goins	(520) 691-4957

STANDARD FORM 298 (REV. 5/2020)
Prescribed by ANSI Std. Z39.18

Contents

List of Figures

List of Tables

1. Introduction

Consolidating powder material through sintering into solid compact geometries is an essential forming process that has two main advantages over casting: 1) enabling consolidation of high melting temperature materials and 2) providing different levers to control microstructural features. However, sintering is often accompanied by numerous challenges that negatively impact the resultant compact.

Sintering is typically time-consuming to achieve completion, and even then, residual porosity may remain. Because the thermal environment is sufficient to facilitate processes like Ostwald Ripening,[1] it is also generally sufficient for curvature-driven motion of grain boundaries, yielding substantial grain growth. Approaches such as solid-state active sintering,[2,3] premelt/liquid-accelerated sintering,[4,5] and hot isostatic pressing[6,7] can engender faster sintering; however, these generally come at the cost of loss of critical microstructural features, loss of geometric control in design, or prohibitive cost. For nanocrystalline systems,[8] sintering acceleration techniques such as these may not preserve the target microstructure.

Recently, a promising new approach called nanophase separation sintering (NPSS) developed by Schuh et al. pressurelessly sinters materials in the solid state rapidly at lower temperatures while preserving microstructure.[9,10] The process involves the formation of a nanostructured phase separation that facilitates the diffusional transport in the system along necks at a lower temperature than other sintering approaches. The advantages of low-temperature sintering without application of pressure are numerous—including reduced cost of necessary manufacturing equipment and energy costs, finer and more-controlled microstructures, reduced cost of production, and more complete sintering processes (resulting in lower risk of defective components). NPSS has been successfully demonstrated in several binary systems (W–Cr, Cr–Ni, Mo–Cr, and Ti–Mg), a few ternary systems (Mo–Cr–W), and higher-order systems (Ni–Cu–Co–Mn, Ni–Cu–Fe–Mn).[9–14]

The foundational works on the rapid separation sintering work identified three preliminary thermodynamic requirements based on the mechanisms at work, which must be met to drive the process for alloy formation:

1) As the name of the NPSS process suggests, the system must have a temperature window of the phase diagram where phase separation will occur. The primary mechanism of this approach is that second phases form along the necks between particles, which accelerate the sintering process; thus, a second phase is necessary. Such phase separation tends to happen at lower temperatures within a given system, but from a practical standpoint

phase separation should happen at a temperature where mass transport is active.[13]

2) The surface energy of the secondary phase should be lower than that of the primary phase to ensure the phase forms on particle surfaces at the necks during sintering. Melting temperature of the phase is used as a proxy for surface energy as it has been shown to be well-correlated with surface energy values.[15] Therefore, the melting temperature of the minority phase should be lower than the base element. This is also anticipated to correlate with superior diffusion rates in the minority species.

3) Schuh et al. specify that there should be good solubility of the base element in the minority phase at the sintering temperature to facilitate fast transport.[9,10] High immiscibility would make the transport slow and greatly diminish any accelerating effect of a minority phase present at the neck. However, recent works comparing the efficacy of the existing experimentally executed systems suggested that the third criteria should be full solubility at high temperatures, rather than just good solubility.[14,16]

These three criteria are based on thermodynamic considerations and can therefore be effectively screened through phase diagram analyses of binary, ternary, and higher-order systems. After these conditions are met, the kinetics of the process should be considered particularly in terms of the industrial feasibility of the processing parameters of a system (i.e., the temperature ranges and their attendant diffusivities).

A rough diffusion criterion for ranking material systems was considered by Naunheim and Schuh[13] based on the interdiffusion at the solidus temperature. The activation energy for sintering was found to agree with the activation energy for diffusion of the secondary component in the primary, which would provide another useful metric in the selection process.[9]

To help assist in this further feasibility estimation, a diffusion-based estimator has been developed as an add-on to the thermodynamics-based primary tool using diffusion curves generated from Thermo-Calc's DICTRA. Unlike thermodynamics data, diffusion data tends to be sparse and reliant on only a handful of data points; thus, its accuracy to multicomponent alloys is relatively poor, but nonetheless this tool will hopefully provide an order-of-magnitude estimator of kinetics behavior for determining feasibility as a starting point for further study.

Overall, it is hoped that this set of modules will provide the basis for further work within the DoD for accelerating alloy development in conjunction with cutting-

edge processing developments for both nanostructured and high-temperature systems.

In this report, a new code package is presented for systematically exploring binary, ternary, and potentially higher-order alloys systems for viability with this approach. The code package is written into a user-accessible Python3 Jupiter Notebook that wraps around the commercially available Thermo-Calc Software Development Kit (SDK) for accessing thermodynamic information about alloy systems.[17,18] The code takes as input a list of elements to explore, as well as a choice of Thermo-Calc database(s), and presents a score for viability of an alloy system with rapid nanophase sintering for combinations of those elements, along with a highlight of compositional and temperature ranges where this process is expected to occur.

2. Methods

Here, a code package has been developed that systematically screens through candidate systems based on the above criteria and selects promising candidates for rapid nanophase sintering. The package is developed in Python 3.10 Jupyter Notebook and uses the Thermo-Calc SDK to perform Thermo-Calc computations on demand as the user-specified problem is executed.[17,18]

The package first takes a list of elements to be studied as input. A user can either focus on a specific base element or prepare a list of elements to study in combinations. For a given elemental combination, the code will create a score map to represent the feasibility of using rapid nanophase sintering at a given composition and temperature. This model considers the majority species the "base" element and the other elements as the "alloying" elements at a given composition point. Thus, a binary phase diagram, for example, will have two regions on the phase diagram divided left and right, where each element is the "base" representing the majority mole fraction of the system.

Three component scores are sequentially generated based on the criteria outlined in Section 1 that are necessary for rapid nanophase sintering.

First, a score is computed for each compositional point in the phase diagram to specify whether a given point satisfied the phase separation requirements or not. Only solid-state phase separation from a miscibility gap or intermetallic compounds satisfy this criterion, and any liquid present is disqualifying. For the phase separation score, a binary 1 or 0 is used (1 if there are at least two solid phases present and 0 otherwise—single phases, liquid present, etc.). At least two solid phases are required to have different base compositions (i.e., an element *i*-rich phase and an element *j*-rich phase). The cutoff parameter to define whether

something is an element-rich phase is currently set at greater than 50% in the code as we are focusing on binary and ternary systems; however, this can be adjusted in the future to reflect compositionally complex alloys or other considerations.

Schuh et al. also cautioned against the formation of intermetallic phases, again citing slow kinetics of diffusion.[9,10] However, it is not guaranteed that all intermetallic compounds will necessarily have poor transport; some intermetallic phases can have a stable range of concentrations sufficient to support a concentration gradient over the width of the precipitated particles. Therefore, in this work, the formation of an intermetallic compound will be considered a point of caution—not outright disqualification—for candidate materials.

The second element of the composite score is melting point differential, which is used as a proxy to surface energy (and may also capture beneficial interdiffusivity properties). The elemental melting points are computed from the phase diagram. For each, the melting point relative differential is used to calculate a score if the base element $T_{M,i}$ melting point is higher than the alloying element melting point $T_{M,j}$:

$$S_{Surface\ Energy\ ij} = \begin{cases} \frac{T_{M,i} - T_{M,j}}{T_{Mi}} & \text{if } T_{M,i} > T_{M,j} \\ 0 & \text{otherwise} \end{cases} \quad (1)$$

Thus, if the proposed sintering aid element melts at a higher point, the score is zero, and if the melting point difference is small, the score contribution will be as well. The greater the difference, the more favorable the formation of the second phase at the point of necking. In contrast to the other scores computed, this score is a single scalar between each set of elements. Future work may refine this model for more direct and accurate evaluations of surface energy and diffusivity by examining the surface energy of each phase as a function of alloy composition. However, melting temperatures are known to be strongly correlated with surface energy values and are easy to calculate.[15]

The third score component is computed from the solubility of the base element in the minority phases for a given temperature. This is computed from the phase diagram for a pair of elements using the concentration that would be present in a saturated second phase particle, which makes it a function of temperature for a given pair of elements. This score component will be nonzero as long as there is finite solubility between the elements in two phases (which is generally true); however, orders of magnitude of difference among them may exist between insoluble and soluble elements.

$$S_{Solubility\ ij} = X_{i\ in\ J} \quad (2)$$

Here, $X_{i \text{ in } J}$ is the concentration if element i in the j-rich phase J. Equation 2 can serve both versions of the solubility criteria—the original high solubility[9,10] and the more recent criterion that there should be full solubility,[14,16] as this score is a scalar.

When all scores are computed for a given multicomponent system, the final score for a given system is computed as a product of the scoring elements. The product is a natural choice for an unparameterized score in a system in which failing to meet any criterion likely makes use of this approach impossible. For ternary and higher component systems one element is considered the base (i) and the sum of the combination of other elements with i is considered. In the event that a base element is alloyed with multiple potential NPSS aid elements, those scores are added together; however, it is likely in practice there are diminishing returns for using multiple sintering aids as they both compete for necking sites. Nonsintering elements added to the system will also affect the composite NPSS score by changing the windows of phase formation, solubility, and so on (they may also affect transport, discussed below), which is an important point of consideration when designing application-driven alloy compositions.

$$S_{Composite\ i} = \sum_{j=0, i \neq j}^{N} S_{Solubility\ ij} \cdot S_{Surface\ Energy\ ij} \cdot S_{Miscibility\ Gap\ ij} \tag{3}$$

This score is calculated at a given temperature, which should be considered as the onset of the temperature window for densification (i.e., the temperature window must start in the two-phase region). A complete determination of the heat treatment parameters should account for the diffusion factors and so on, as shown in Figure 1. The score calculated in Equation 3 is meant for screening; for each elemental combination, a diagram may be computed, and a peak score is also used to quickly sort through potential candidates using the maximum value identified anywhere in the phase diagram for the multicomponent system. The score diagrams may be used for specific alloy and sintering temperature selections. However, recall that scores are unparameterized and do not consider kinetics or other design considerations; therefore, expert guidance should be used to decide final compositions and temperatures for a given system with the calculated score as just one consideration.

3. Results and Discussion

We first work through an illustrative example of a successful NPSS as found in literature and then extend to some refractory multicomponent systems (Mo and W). We use the TCHEA4 database in Thermo-Calc throughout.

The experimentally demonstrated Cr–Ni binary system[9] is considered with Fe added as a tertiary alloying additive to demonstrate the visualization of ternary alloys. Tertiary alloying elements may offer advantages over the binary in improved diffusion or other processing considerations, while moderately affecting the phase diagram. A ternary diagram of the calculated score from Equation 3 for the Cr–Ni–Fe system is shown in Figure 1a. Each component score is computed for every element, resulting in the contour plot indicating compositional regions of interest. As can be seen in Figure 1, the experimentally observed composition, indicated by the green star, is in a high score region. In order To more thoroughly discuss the score determination, we consider a set Fe composition of 5at% as shown by the cyan dashed line on Figure 1a. The pseudo-binary phase diagram of Cr–Ni–5at%Fe is shown in Figure 1b.

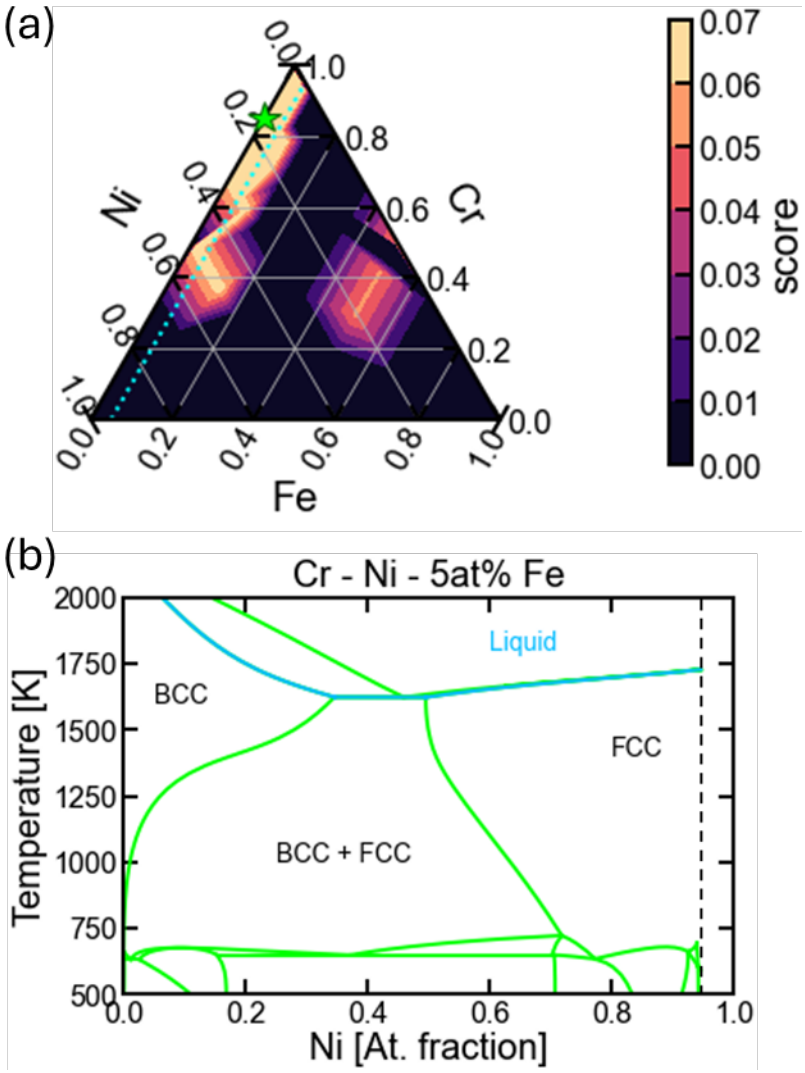

Figure 1. (a) Ternary diagram of the sintering score as a function of composition at 1050 K. Successful experimental system[9] denoted by green star. (b) Calculated phase diagram of example Cr–Ni–Fe system at 5% atomic Fe concentration. The pseudo-binary slice is indicated by the cyan dotted line on the ternary.

The pseudo-binary phase diagram is overlaid on the sintering scores in Figure 2. Starting with the surface energy score, it is seen that Cr is the higher melting point element, and the melting point (and therefore, the surface energy) decreases as Ni is added. The score is nonzero when the majority element is Cr; however, Ni as the base element and Cr as the sintering aid would be unlikely to work due to surface energy considerations. Figure 2b shows the two-phase region score, where two suitable phases are computed to exist. The actual two-phase region as defined by the pseudo-binary diagram extends to higher temperatures than the two-phase region score indicates. This is due to the criteria requiring that one of the two phases be majority element *i* (i.e., Cr) and the second be majority atomic fraction element

j (i.e., Ni). The addition of a ternary element can therefore reduce the *suitable* two-phase region even if the phase diagram is less affected; it also adds some complicating phases around 700 K, which the model suggests avoiding for low-Cr concentrations, but otherwise still predicts favorable outcomes in this example. The Minority Phase Solubility score in Figure 2c shows that both Ni and Cr are fairly miscible with one another's primary phases in a large temperature window, especially above 1000 K. Figure 2d is the composite score, which includes all considerations, showing regions predicted where NPSS is still likely to occur even with 5% added Fe.

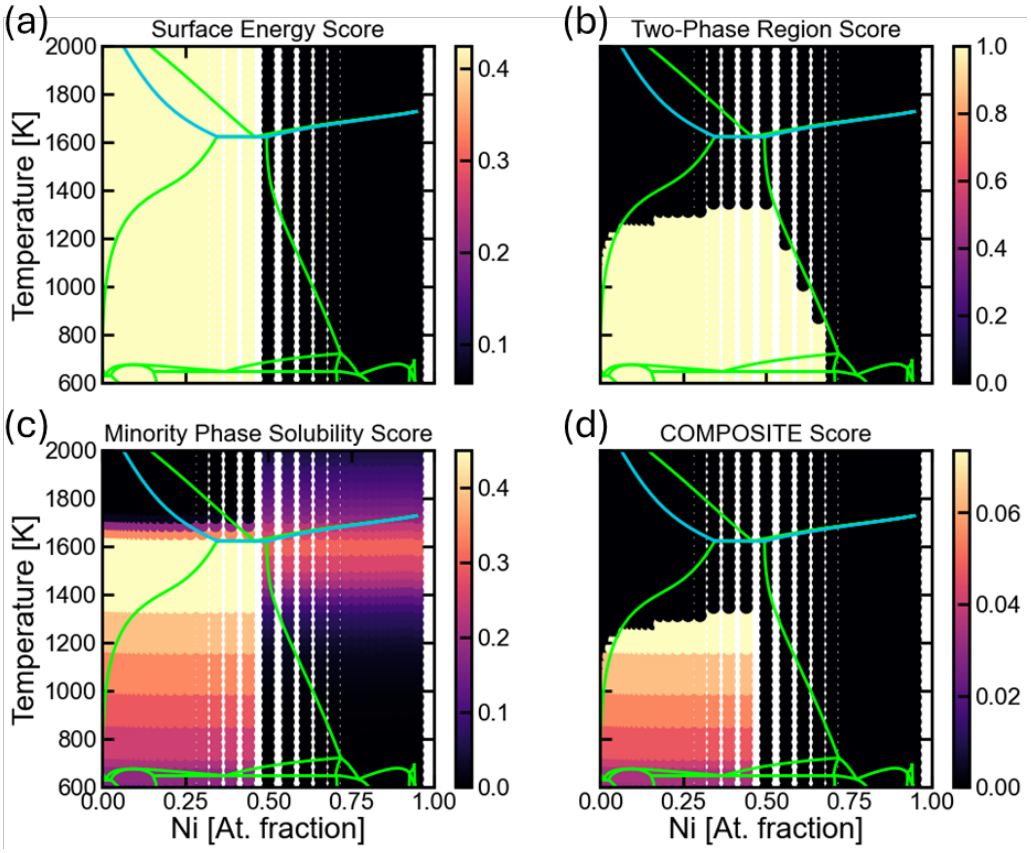

Figure 2. (a) Melting temperature-derived surface energy score. (b) Two-phase region (miscibility gap) score. (c) Base element solubility in minority phase score. (d) Overall composite score for the Cr–Ni–Fe system, fixing Fe at 5% atomic concentration.

The experimentally successful W–Cr,[9] Mo–Cr,[14] and Mo–25W–15Cr[12] can all be demonstrated on a ternary score plot (Figure 3, shown at 900 K). The original W–Cr system is deemed most promising of these three, but all have strong nonzero scores and are thus predicted to be promising candidates for the approach. Given that the score is unparametrized, any score greater than zero can be considered; however, it is expected that comparatively low scores will perform worse in practice than higher-scoring compositions, especially within a given ally system.

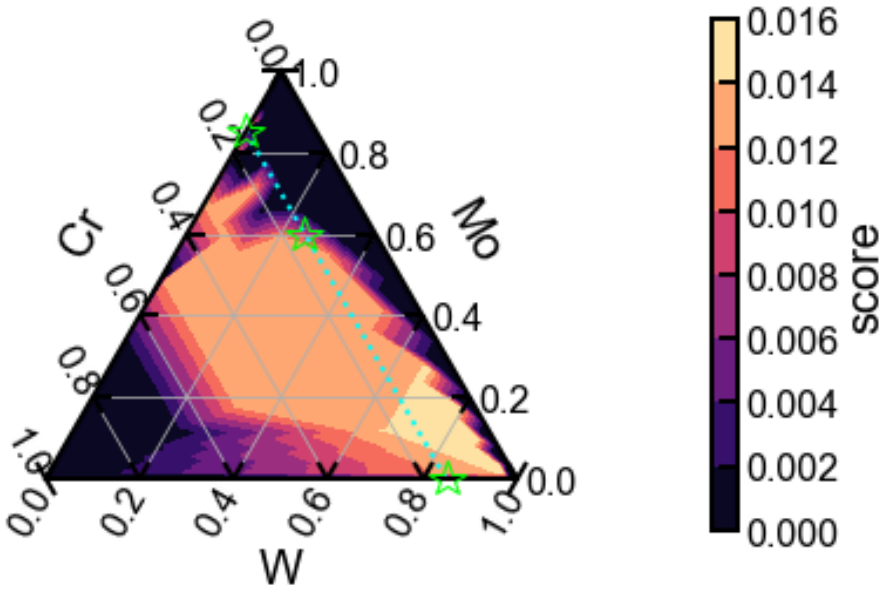

Figure 3. Mo–Cr–W system score ternary at 900 K; experimentally confirmed systems (W–Cr, Mo–Cr[20], Mo–25W–15Cr[14]) are indicated by stars.

Two positive and one negative ternary example systems are shown in Figure 4; most systems such as the one in Figure 4a have no regions of potential for NPSS at all. Table 1 lists some representative nonexhaustive examples of candidate materials (including some experimentally demonstrated systems) for Mo- and W-based alloy systems. Mo and W have some known experimental systems, so ensuring those are reproduced here can test the model validity.

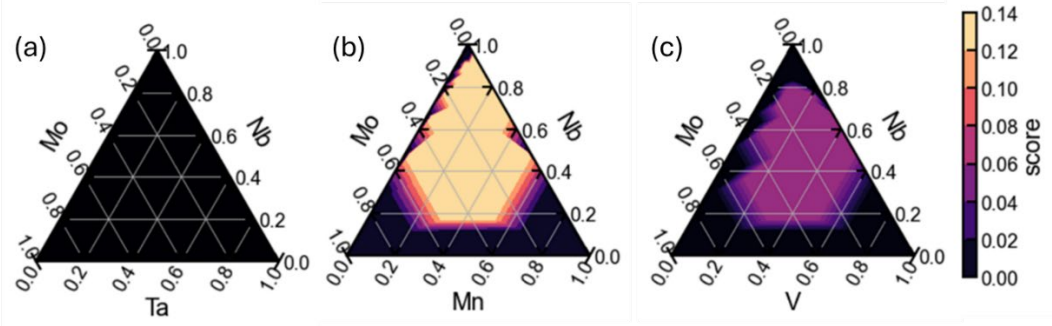

Figure 4. Score plots for the (a) Mo–Nb–Ta (at 1250 K), (b) Mo–Nb–Mn (at 1250 K), and (c) Mo–Nb–V (at 550 K) system.

Table 1. List of example alloy systems identified as NPSS candidates, emphasizing Mo and W in order of base element and then score.

Example predicted alloys	
Mo–Cr[a]	W–Cr[a]
Mo–V	W–Ni
Mo–Ru	W–Ru
Mo–Fe	W–Fe
Mo–Ni	W–Co
Mo–Nb–V	W-Mo-Mn
Mo–Nb–Mn	W–Ni–Cr[a]
Mo–W–Cr[a]	W–Ti–Fe
Mo–Ru–Co	W–Fe–Mn

[a] Previous experimentally verified systems.

As mentioned previously, two main benefits of the NPSS method are potentially to preserve nanostructure during sintering or facilitate high melting materials; in this work we focus on some high melting point material surveys as alloy design for nanostructure. A number of refractory ternary systems have been tested with this approach as preliminary examples of candidate materials. They will not be listed here exhaustively, as ongoing experimental efforts are being made to validate the materials as future work, and over 100 binary or candidates were identified between Mo and W alone (many of which are simple derivatives of binaries—i.e., nearly every ternary including the strong candidate W–Cr was also itself a candidate). However, some interesting representative examples are shown in Figure 4. Many systems do not have regions of nonzero scores such as Mo–Nb–Ta. (In particular, Mo–Nb–Ta has a zero score because of complete solubility—e.g., no second phase regions.) Oliver and Schuh[14] noted that the Mo–Nb system only meets two out of three criteria, not having two-phase solubility. This is reflected in the Mo–Nb–Mn and Mo–Nb–V system diagrams in Figure 4 where the Mo–Nb side of the ternary has a region of zero score, followed by a sharp increase to high scores with the addition of Mn or V. The tertiary element provides the necessary phase separation, which can be seen more clearly via the pseudo-binary slices in Figure 5.

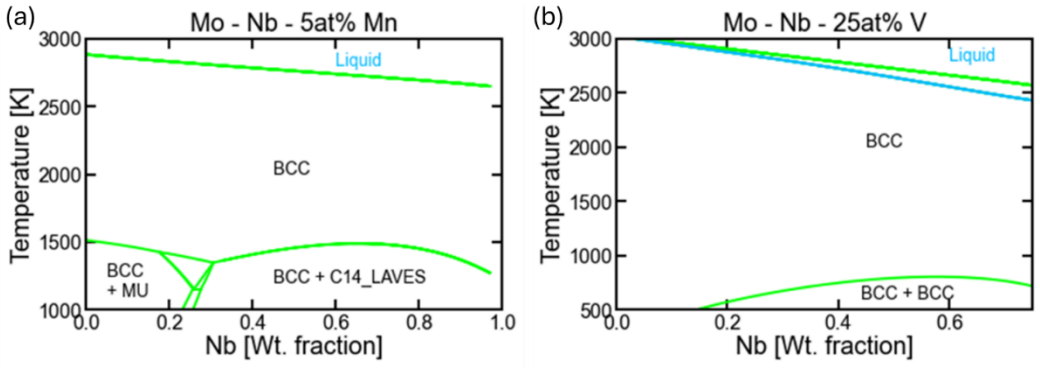

Figure 5. Pseudo-binary phase diagrams for (a) Mo–Nb–5at%Mn and (b) Mo–Nb–25%V.

In prior work on NPSS, intermetallics were not considered due to questions about their ability to provide effective diffusion pathways. There is very limited data on diffusion in intermetallic phases, but some have the potential to facilitate diffusion, so we have not ruled them out in this study.[19] When observing the Mo–Nb–Mn pseudobinary diagram we see that all the two-phase regions involve intermetallics.

The MU phase listed in Figure 5a represents μ-Mn_7Mo_6; C14_LAVES specifies Laves Mn_2Nb. Considering diffusion in intermetallics, if Mo diffusion is desired, one would select compositions that form the μ phase; if diffusion of Nb is desired, formation of Laves phases should be targeted. Future experimental study is planned to test the viability of intermetallics in serving as the second phases in the NPSS approach. In contrast, the Mo–Nb–V system is more typical with a phase separating body-centered cubic (BCC) regions at low temperatures.

Removing any false positives is the larger and ongoing challenge with this package. How to identify systems that have satisfactory thermodynamic conditions is known; however, it is possible that the kinetics or microstructural features in some of these systems may in some way inhibit the rapid nanophase separation sintering process and make it difficult to realize in practice.

Other considerations could also be used, such as general material design constraints including predicted properties, use of binders, cost, etc. Alloy design tool effectiveness improves when used in conjunction with one another and the design space is reduced to a small number of candidates for detailed evaluation. This tool is intended to be used in combination with alloy design criteria. The kinetics of a system should be considered as it is almost as critical in governing consolidation processes as thermodynamics. To that end, an add-on to this filter has been developed to provide cursory information to guide this selection (discussed in Section 4).

Other filters or weights can be used to facilitate alloy design as future work. For example, the requirements for nanophase sintering can yield either stable nanoscale microstructures (i.e., W–Cr), or transient nanoscale structures that grow toward micron-scale grains after processing (i.e., Ni–Cr). This depends on segregation to grain boundaries as a feature, and other efforts have been made to identify those alloy systems at U.S. Army Combat Capabilities Development Command Army Research Laboratory and elsewhere.[8,20] The modular nature of the notebook allows any user-defined objective function to be easily added into these tools (or for these tools to be integrated into another user's workflow).

4. Diffusion-Driven Kinetics Estimator

The phase diagrams and thermodynamics of many material systems of interest are reasonably well-defined (i.e., with the emergence of high entropy alloys resulting in a rapid development of ternary and higher-order multicomponent phase diagrams to be constructed)[21,22]; however, system kinetics remain an area with far less available systematic data. Nonetheless, an add-on module that provides some rough estimator of feasibility has been written as an additional feature to help in the alloy selection and sintering temperature selection process. It uses the Thermo-Calc DICTRA platform to estimate diffusive behavior. Diffusion coefficients are themselves a function of composition, and in multicomponent systems they become an increasingly large tensor as the number of elements increases. Thermo-Calc software does not store diffusion coefficient tensors themselves, and there is no straightforward way to export them directly for complex compositions.[17,18]

To compute diffusion coefficients from Thermo-Calc as a function of temperature and composition, user-defined multicomponent diffusion couples are set up, and the diffusion coefficients are computed from the time series data of the diffusion couple at each point. As mentioned previously, the work on NPSS indicates that the redissolution of the particles formed into the necks provides the advanced transport mechanism in at least some systems (e.g., the Mo–Cr system).[14] Here, the module contains two parts: the first creates some user-defined diffusion profile calculation in a multicomponent system and the second calculates the diffusion coefficients and activation energies from those DICTRA calculation outputs. The first TC-Python SDK notebook sections straightforwardly execute Thermo-Calc calculations to compute the primary stable phase present at a particular composition and temperature using a single equilibrium calculation to identify the phases present, their proportions, and the atomic composition of each phase. The highest mole fraction phase is considered the dominant phase when more than one phase is predicted to be stable.

The package then executes a diffusion time series within this phase to create transport data in a manner consistent with the model's requirements. A diffusion couple within a single phase is set up as a single region, with a step in composition. The package uses a single region in one dimension with a composition step halfway through, between a space in the base alloy where there is a small amount of sintering aid on one side, and none on the other, while preserving the molar ratio within the balance base alloy. The user must specify a sintering temperature (in Kelvin), the system length scale (in meters), and the simulation time (in seconds); however, the TC-Python SDK notebook provides example values. The package will automatically export the diffusion time series data into a Microsoft Excel notebook

with the appropriate data, file name, and column headers for further use, which also ensures a "save point" that mitigates the risk of data loss in the event of program interruptions. To compute activation energies and vibrational diffusion prefactors, a second run at a different temperature must be conducted, which the code package will automatically perform for the user.

The second section of the kinetics module in the Python notebook uses these outputs to generate diffusion data from the diffusion profiles. The user selects the elements of interest and the temperatures to query. The notebook then performs the necessary steps to compute the diffusion coefficient D (at a given temperature) and the activation energy Q, which are useful quantities to measure to determine the kinetic rate at which sintering and other densification processes may occur for a set of conditions. The method of extracting these values from DICTRA-generated curves is straightforward using Fick's laws.[23] Particularly, Fick's Second Law can be expressed as

$$\frac{d\varphi}{dt} = D\frac{d^2\varphi}{dx^2} \tag{4}$$

Thus, D can be computed by numerically differentiating the diffusion time series composition profiles and using those values here.

Theoretically, D should be solved for as a fairly flat value (with some variation based on composition if you were to vary it significantly across the step; Figure 6); however, because the sign changes along the time derivative (and second derivative with respect to position) and intersects zero, division by zero makes this point undefined and the area around it is very noisy for numerical reasons. There also tends to be larger error around Thermo-Calc's fixed boundaries due to the numerical approach used in their software. Therefore, values of the estimate of D are taken as the median from regions where the derivatives are largest in magnitude and at least 10 steps away from the system bounds. Values of activation energy Q are taken by computing D at two or more temperatures. Q represents the energetic barrier to the atomic process that underpins diffusion (and other thermally activated processes) as

$$D = D_0 e^{\frac{-Q}{RT}} \tag{5}$$

where D_0 is a frequency and geometric-based prefactor and R is the gas constant. It is common in thermally activated processes to compute Q from the slope of the line between the log of the property measured (here, D) against $1/T$.

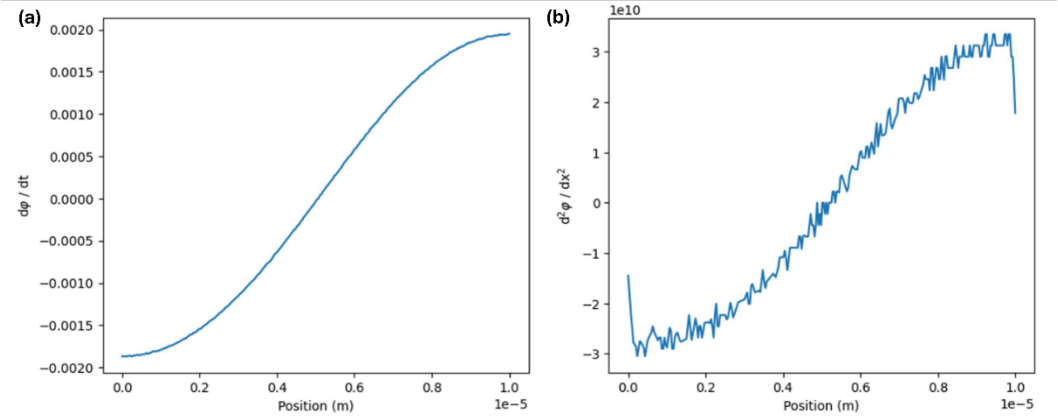

Figure 6. (a) Time and (b) spatial derivatives of composition after a period of diffusion in FeNi as an example.

An example of this workflow was tested against the Fe–Ni system (as shown in Figures 1–6), which is a well-studied alloy where values have been measured by multiple authors for Ni in a BCC Fe matrix. Here, the module computes an activation energy value Q of 230.2 kJ/mol, compared to the NIST's tabulated values of 234 kJ/mol, and a vibrational prefactor D_0 of 1.1 10^{-4} m^2/s versus the NIST tabulated value of 1.3 10^{-4} m^2/s (taken from Averbach et al., which is in very close agreement).[24,25] This demonstrates at least that this approach can suitably derive diffusion coefficients from Thermo-Calc for some arbitrary composition and conditions. These values likely have greater inaccuracy depending on the level of data for a given system. However, we hope that these will give approximate values or at least order-of-magnitude guidance that can be used to inform the starting point for an experimental study or advise which alloy systems to prioritize or avoid. More importantly, it can estimate the diffusion in couples with more-complex compositions than binaries. Table 2 lists example systems where the final element named in an alloy is the one that is directly measured for a given diffusion coefficient.

Table 2. Example computed diffusion data from kinetics sub-module.

Alloy	D_0 (m^2/s)	Q (kJ/mol)
Fe–Ni	1.13E-04	230
Mo–Cr	3.81E-05	224
Nb–Cr	1.17E-06	190
Nb–Mn	1.43E-04	219
Nb–Mo	1.03E-03	471
Nb–V	8.78E-04	229
Nb–Zr	8.54E-05	377
Ta–Ti	9.30E-05	211
V–Cr	1.11E-06	190
Zr–Mn	2.10E-04	222
Nb–Zr_1–Mn	1.92E-04	222
Nb–Zr_2–Mn	2.04E-04	223
Nb–Zr_3–Mn	1.09E-04	216
Nb–Zr_4–Mn	9.47E-05	214
Nb–Zr_5–Mn	1.24E-04	217
Nb–Zr_{10}–Mn	2.29E-04	224
Nb–Zr_{15}–Mn	7.46E-05	212
Nb–Zr_{20}–Mn	8.87E-05	214
Nb–Zr_{25}–Mn	1.23E-04	217
Nb–Mo_1–V	6.49E-09	247
Nb–Mo_{10}–V	3.66E-11	172
Nb–Mo_{20}–V	4.47E-10	213
Nb–Mo_1–Cr	5.66E-05	218
Nb–Mo_5–Cr	1.91E-05	208
Nb–Mo_{10}–Cr	1.78E-05	207
Nb–V_1–Cr	5.96E-06	204
Nb–V_5–Cr	6.87E-06	205
Nb–V_{10}–Cr	2.75E-06	197
Nb–V_{20}–Cr	1.16E-04	228

Because the specific configurations of a sintering system depend strongly on user needs, whether a particular alloy's diffusion parameters are satisfactory or not depends on the precursor physiology and sintering temperature window desired and cannot be decided based on the code here, as temperature and time requirements may vary widely. However, having the values on hand for an alloy can allow alloy design efforts to gauge feasibility in conjunction with other potential requirements. Kinetics databases such as the MOBHEA2 from Thermo-Calc used in this work are far less developed than thermodynamic databases and may be missing parts of the composition space or extrapolating others; therefore, users must exercise discretion in the level of trust given to a particular value or ideally confirm with experimental literature if extant.

For example, the Nb–Mo–V system was identified as a potential candidate based on the three thermodynamic criteria used to compute the score; however, as seen in Table 2 the diffusion prefactor is many orders of magnitude lower than the successful experimentally observed Mo–Cr system. Another ternary system with

positive scores (Nb–Mo–Cr) has diffusion values more in line with the experimental system. These values could also be used in a more-rigorous version of the interdiffusion criteria found in Naunheim and Schuh[13] if designed by the user. However, these values are computed for bulk system diffusion. In some cases, the desired microstructure will be nanocrystalline, in which case grain boundary diffusion may provide the dominant transport mechanism rather than bulk diffusion at comparatively lower temperatures, which may mean some systems with poor bulk diffusion may still be viable candidates—particularly, if the grain boundaries are stabilized at and below the sintering temperature. In some systems, with proper calibration, bulk diffusion can still be a useful property in surrogate models to predict grain boundary diffusion. A very rough first estimate is that grain boundary diffusion in metals has a similar prefactor and often has activation energy of 0.4–0.6 the bulk value.[26] In all cases, the user must at a minimum understand a starting microstructure, sintering temperature, and bulk diffusion properties to estimate which modes of transport are active to gauge the overall expected kinetics of their system.

5. Conclusions

A package to identify candidate multicomponent systems that undergo rapid nanophase sintering has been developed. Rapid nanophase separation sintering is a recently identified approach to accelerate the sintering process of materials, using the formation of second-phase particles at necks during sintering to enhance transport. Several thermodynamic criteria must be met, which are evaluated by this code for a given material system or list of material systems. Materials are scored based on the theoretical thermodynamic capability of using this approach. This approach has correctly identified the NPSS systems shown in literature. Numerous new binary and ternary alloys have been identified as potential candidates, which are in the process of being validated—particularly, in the case of phase separating systems involving intermetallic phases. Further, a rudimentary system for gauging kinetics of screened systems has also been written to accompany the thermodynamics-based system. We expect this toolset to assist in alloy design of materials that can be sintered solid-state at low temperatures as part of the material selection process and used to enhance the rapid sintering process through composition and temperature optimization as one part of the alloy design process within a range of DoD component materials design or engineering programs.

6. References

1. Ostwald W. Studies on the formation and transformation of solid bodies. Zeit Physik Chemie. 1897;22:289–330.
2. Johnson JL, German RM. Theoretical modeling of densification during activated solid-state sintering. Metal & Mater Trans A. 1996;27:441–450.
3. Gupta VK, Yoon D, Meyer III HM, Luo J. Thin intergranular films and solid-state activated sintering in nickel-doped tungsten. Acta Mater. 2007;55(9):3131–3142.
4. German RM, Suri P, Park SJ. Review: liquid phase sintering. J Mater Sci. 2009;44:1–39.
5. Svoboda J, Riedel H, Gaebel R. A model for liquid phase sintering. Act Mater. 1996;44(8):3215–3226.
6. Atkinson HV, Davies S. Fundamental aspects of hot isostatic pressing: an overview. Metal & Mater Trans. A. 2000;31:2981–3000.
7. Schoell R et al. Hot isostatic pressing control of tungsten-based composites. Inorganics. 2023;11(2):82.
8. Hammond VH et al. Processing of bulk nanocrystalline metals at the US Army Research Laboratory. J Vis. Exp. 2018;133:56950.
9. Park M, Schuh CA. Accelerated sintering in phase-separated nanostructured alloys. Nature Comm. 2015;6:6858.
10. Park M, Chookajorn T, Schuh CA. Nano-phase separation in nanostructure-stable vs. bulk-stable alloys. Acta Mater. 2018;145:123–133.
11. Graetz K, Paras JS, Schuh CA. Nanostructure stability and nano-phase separation in the titanium magnesium system. Materialia. 2018;1:89–98.
12. Oliver C, Schuh CA. Design of a rapidly sintering Mo-W-Cr alloy. J Alloy and Comp. 2023;938:168492.
13. Naunheim Y, Schuh C. Multicomponent alloys design to sinter. Nature Comm. 2024;15:8028.
14. Oliver C, Schuh CA. Optimization of the Mo-Cr binary system for nanophase separation sintering. Materialia. 2022;22:101410.

15. Reynolds Jr CL, Couchman P. On the relation between surface energy, melting temperature, and interatomic separation for metals. Phil Mag A. 1976;34(4):659–661.

16. Oliver C, Schuh CA. The structural evolution and densification mechanisms of nanophase separation sintering. Metallurgical and Materials Transactions A. 2021;52:4946–4956.

17. Andersson JO, Helander T, Höglund L, Shi PF. Sundman B. Thermo-calc and DICTRA, computational tools for materials science. Calphad. 2002;26:273–312. V. 2025A

18. The TC-Python API programmer guide. Thermo-Calc Software; 2022 Jan 3. https://thermocalc.com/support/documentation/

19. Mehrer H. Self-diffusion, solute-diffusion and interdiffusion in binary intermetallics. Diffusion Foundations. 2014;2:1–72.

20. Chookajorn T, Murdoch HA, Schuh CA. Design of stable nanocrystalline alloys. Science. 2012;337:951–954.

21. Zhang F et al. An understanding of high entropy alloys from phase diagram calculations. Calphad. 2014;45:1–10.

22. Chen HL, Mao H, Chen Q. Database development and calphad calculations for high entropy alloys: Challenges, strategies, and tips. Mater Chem & Phys. 2018;210:279–290.

23. Fick A. On liquid diffusion. Ann Physik & Chemie. 1855;94:59.

24. Marsh T, Lindwall G, Kattner U, Campbell C. Impurity diffusion data, center for theoretical and computational materials science. National Institute of Standards and Technology [accessed 2025 Mar 1]. https://www.ctcms. nist.gov/~gkl/selfdiffusion.html

25. Hirano K, Cohen M, Averbach BL. Diffusion of nickel into iron. Acta Mater. 1961;9(5):440–445.

26. Herzig C, Mishin Y. Grain boundary diffusion in metals. In: Heitjans P, Kärger J. Diffusion in Condensed Matter. Springer, 2005, Chapter 8. ISBN: 978-3-540-20043-7.

List of Symbols, Abbreviations, and Acronyms

ARL	Army Research Laboratory
BCC	body-centered cubic
Cr	chromium
DEVCOM	U.S. Army Combat Capabilities Development Command
DoD	Department of Defense
Fe	iron
Mn	manganese
Mo	molybdenum
Nb	niobium
Ni	nickel
NPSS	nanophase separation sintering
SDK	Software Development Kit
V	vanadium
W	tungsten

1 (PDF)	DEFENSE TECHNICAL INFORMATION CTR DTIC OCA
1 (PDF)	DEVCOM ARL FCDD RLB CI TECH LIB